Raman scattering from the misfit-layer compounds $SnNbS_3$, $PbNbS_3$, and $PbTiS_3$

M. Hangyo,* S. Nakashima, Y. Hamada,† and T. Nishio
Department of Applied Physics, Faculty of Engineering, Osaka University, 2-1 Yamadaoka, Suita, Osaka 565, Japan

Y. Ohno
Department of Physics, Faculty of General Education, Utsunomiya University, 350 Mine-machi, Utsunomiya, Tochigi 321, Japan
(Received 24 September 1992; revised manuscript received 7 June 1993)

Raman-scattering experiments have been carried out on misfit-layer compounds MTS_3 (M=Sn, Pb; T=Nb, Ti), in which two types of building layers, MS and TS_2, are stacked alternately. The spectra obtained from these compounds are regarded as the superposition of the intralayer vibrations of individual layers, which indicates a weak interlayer interaction. The observed Raman shift of the intralayer modes of NbS_2 relative to those of 2H-NbS_2 is interpreted in terms of a charge transfer from the MS layer to the NbS_2 layer.

I. INTRODUCTION

Misfit-layer compounds MTS_3 (M=Sn, Pb, Bi; T=Nb, Ta, Ti, V, Cr) consist of two types of atomic layers, MS and TS_2, stacked alternately along the c axis.[1] The MS layer consists of twofold atomic sheets with a distorted NaCl structure. The TS_2 layer has the same structure as the transition-metal disulfides, in which each metal atom T is surrounded by six S atoms octahedrally or trigonal prismatically. These compounds can be regarded as transition-metal disulfides TS_2 intercalated with the MS layers between van der Waals gaps, and are also considered as one-dimensional superlattices with an extremely short period. The lattice constants of the two layers (MS and TS_2 layers) are the same for the b direction but different for the a direction, giving the incommensurate structure and the accurate formula of $M_{1+x}TS_3$ ($x>0$). This partial lattice matching may cause the strain in the ab planes of the MS and TS_2 layers.

The electrical properties of MTS_3 are quite anisotropic and reflect its layer structure.[1-3] The electronic spectra [x-ray photoemission spectroscopy, x-ray absorption spectroscopy, and reflection-electron energy-loss spectroscopy (XPS, XAS, and REELS)] are interpreted basically in terms of the superposition of those of the MS and TS_2 layers indicative of a weak interlayer interaction.[4] From the detailed analysis of these spectra, it was concluded that a charge transfer from the MS layer to the TS_2 layer occurs.

To our knowledge, there has been no study on the vibrational structure of MTS_3 so far. This paper reports the Raman spectra of MTS_3 ($SnNbS_3$, $PbNbS_3$, and $PbTiS_3$) and their temperature dependence. The purpose of this study is to clarify the relationship between the crystal structure and the vibrational spectra. The obtained spectra are interpreted approximately in terms of the superposition of those of the intralayer modes of the MS and TS_2 layers. Discussions are given on the interlayer interaction and the charge transfer from the MS layer to the TS_2 layer.

II. SYMMETRICAL CONSIDERATION OF VIBRATIONS

The MTS_3 crystals are composed of two sublattices, MS and TS_2 layers, which have lattice constants a_1 and b_1, and a_2 and b_2, respectively, in the ab plane. The lattice constants for the two sublattices within the basal plane (ab plane) are the same for the b direction ($b_1=b_2$), whereas those in the a direction are different ($a_1\neq a_2$). The ratio of the a lattice constants for the two sublattices is irrational and, therefore, the crystal structure is incommensurate. In what follows, for simplicity we assume that the MS layer has tetragonal symmetry (D_{4h}) because the difference between the lattice constants for the a and b directions is less than 2% for the MS layer.[1] In this approximation the primitive unit cell contains two formula units of MS, and then the primitive translation vectors in the ab plane are given by $\mathbf{a}_1'=(\mathbf{a}_1+\mathbf{b}_1)/\sqrt{2}$ and $\mathbf{b}_1'=(\mathbf{a}_1-\mathbf{b}_1)/\sqrt{2}$ as shown in Fig. 1(a). Further, since the deviation of the layer symmetry of the TS_2 layer from the trigonal symmetry is less than 2%,[1] we regard the structure of the TS_2 layer as being the same as 2H-NbS_2 (D_{3h}) for $SnNbS_3$ and $PbNbS_3$, or as 1T-TiS_2 (D_{3d}) for $PbTiS_3$. The primitive translation vectors are $\mathbf{a}_2'$ and $\mathbf{b}_2'$ as shown in Fig. 1(b).

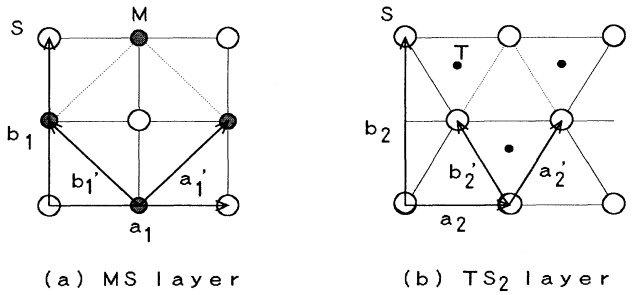

FIG. 1. Simplified structures of (a) MS and (b) TS_2 layers and the primitive unit cells used in the group-theoretical analysis of vibrational modes. Each layer is viewed perpendicular to the basal plane.

Under the assumption of the simplified symmetry, the vibrational modes of the MS layer are decomposed into the following irreducible representations at the Γ point:

$$\Gamma(MS)=2A_{1g}+2E_g+2A_{2u}+2E_u \ , \tag{1}$$

where Raman active modes are $2A_{1g}+2E_g$. The Raman tensors corresponding to the A_{1g} and E_g species of the D_{4h} point group referred to the a_1', b_1' [see Fig. 1(a)], and c axes are given by

$$A_{1g}=\begin{bmatrix} a & 0 & 0 \\ 0 & a & 0 \\ 0 & 0 & b \end{bmatrix} ,$$

$$E_g=\begin{bmatrix} 0 & 0 & f \\ 0 & 0 & 0 \\ g & 0 & 0 \end{bmatrix} , \quad \begin{bmatrix} 0 & 0 & 0 \\ 0 & 0 & f \\ 0 & g & 0 \end{bmatrix} .$$

On the other hand, the vibrational modes of the TS_2 layer are decomposed into the following irreducible representations at the Γ point:

$$\Gamma(NbS_2)=A_1'+2A_2''+2E'+E'' \ , \tag{2}$$

$$\Gamma(TiS_2)=A_{1g}+E_g+2A_{2u}+2E_u \ , \tag{3}$$

where the Raman active modes are $A_1'+E'+E''$ for NbS_2 and $A_{1g}+E_g$ for TiS_2. The Raman tensors corresponding to the A_1', E', and E'' species of the D_{3h} point group referred to the a_2, b_2 [see Fig. 1(b)], and c axes are given by

$$A_1'=\begin{bmatrix} a' & 0 & 0 \\ 0 & a' & 0 \\ 0 & 0 & b' \end{bmatrix} ,$$

$$E'(a_2)=\begin{bmatrix} 0 & c' & 0 \\ c' & 0 & 0 \\ 0 & 0 & 0 \end{bmatrix} , \quad E'(b_2)=\begin{bmatrix} c' & 0 & 0 \\ 0 & -c' & 0 \\ 0 & 0 & 0 \end{bmatrix} ,$$

$$E''=\begin{bmatrix} 0 & 0 & 0 \\ 0 & 0 & d' \\ 0 & d' & 0 \end{bmatrix} , \quad \begin{bmatrix} 0 & 0 & -d' \\ 0 & 0 & 0 \\ -d' & 0 & 0 \end{bmatrix} ,$$

and those corresponding to the A_{1g} and E_g species of the D_{3d} point group referred to the a_2, b_2, and c axes are given by

$$A_{1g}=\begin{bmatrix} a'' & 0 & 0 \\ 0 & a'' & 0 \\ 0 & 0 & b'' \end{bmatrix} ,$$

$$E_g=\begin{bmatrix} c'' & 0 & 0 \\ 0 & -c'' & d'' \\ 0 & d'' & 0 \end{bmatrix} , \quad \begin{bmatrix} 0 & -c'' & -d'' \\ -c'' & 0 & 0 \\ -d'' & 0 & 0 \end{bmatrix} .$$

The slight anisotropy of the ab plane may induce the small splitting of the E modes.

III. EXPERIMENT

Single crystals of $SnNbS_3$, $PbNbS_3$, and $PbTiS_3$ were grown by the chemical-vapor transport method.[4] Structural and chemical analysis were performed by means of the x-ray powder diffraction method and the XPS technique. All diffraction peaks observed were well indexed using the lattice constants in Ref. 1. Chemical compositions are also consistent with those reported in Ref. 1 within experimental errors. Thin platelike specimens several mm^2 in area were used for the Raman-scattering measurements. The Raman-scattering measurements were made in the quasibackscattering geometry with the exciting wavelength of 5145 or 4880 Å of an Ar ion laser. The scattered light was dispersed by a double monochromator and detected by a standard photon counting system. The samples were mounted on a cold finger of a closed-cycle helium refrigerator for the measurements at low temperatures.

IV. RESULTS AND DISCUSSION

A. Raman spectra of $SnNbS_3$, $PbNbS_3$, and $PbTiS_3$

Figure 2 shows Raman spectra of $SnNbS_3$, $PbNbS_3$, and $PbTiS_3$ measured at room temperature. The spectra of $2H$-NbS_2 and its intercalation compound $NbS_2(pyridine)_{1/2}$, and $1T$-TiS_2 are also shown for comparison. Figure 3 shows the polarization dependence of the spectra. The notations (XX) and (XY) refer to the polarized and depolarized spectra, respectively. The X and Y directions lie in the ab plane, but the relation between the X and Y directions and the a and b crystal axes is not specified in this experiment. For $SnNbS_3$, peaks appear at 370 ± 2 and 335 ± 3 cm^{-1} in the (XX) spectrum and at 335 ± 3 cm^{-1} in the (XY) spectrum in the frequency region above 300 cm^{-1}. Similarly, peaks appear at 374 ± 2 and 340 ± 3 cm^{-1} in the (XX) spectrum and at 340 ± 3 cm^{-1} in the (XY) spectrum for $PbNbS_3$. Nakashima *et al.*[5] and McMullan and Irwin[6] assigned the peaks at 379 and 309 cm^{-1} (304 cm^{-1} in Ref. 6) of $2H$-NbS_2 to the A_{1g} and E_{2g} modes, respectively. The primitive unit cell of $2H$-NbS_2 contains two NbS_2 layers and its space group is D_{6h}^4. The A_{1g} and E_{2g} modes of $2H$-NbS_3 correspond to the A_1' and E' modes in the D_{3h} symmetry, respectively. For the A_{1g} mode the S atoms are displaced perpendicular to the basal plane and for the E_{2g} mode the Nb and S atoms are displaced parallel to the basal plane with an opposite phase. Since the structure of the NbS_2 layer in $SnNbS_3$ and $PbNbS_3$ is almost the same as those of $2H$-NbS_2 except for a slight distortion, the frequencies and polarization dependence of the modes corresponding to the intralayer vibration of the NbS_2 layer in these crystals may be similar to those of $2H$-NbS_2. The peak frequencies of 370 (374) and 335 (340) cm^{-1} of $SnNbS_3$ ($PbNbS_3$) are close to the frequencies of 379 (A_{1g}) and 309 cm^{-1} (E_{1g}) of $2H$-NbS_2, respectively. The polarization measurements show that the modes at 370 (374) cm^{-1} and 335 (340) cm^{-1} have the A_{1g} and E_{2g} characteristics, respectively, as seen in Fig. 3. Further, the phonon modes of the SnS and PbS layers in MTS_3 are expected to appear below 300 cm^{-1} as will be discussed later. From the above consideration, we assign the 370 (374) and 335 (340) cm^{-1} lines to the A_1' (A_{1g}) and E' (E_{2g}) modes, respectively, in the NbS_2 layer. Broad bands at around 290 cm^{-1} seen in both $SnNbS_3$ and

$PbNbS_3$ spectra are assigned to the second-order scattering as for $2H$-NbS_2.[5]

A similar discussion can be applied to the spectra of $PbTiS_3$. The 335 and 235 cm^{-1} lines observed for the $1T$-TiS_2 crystal were assigned to the A_{1g} and E_g modes, respectively, of the TiS_2 layer by Smith *et al.*[7] The 329±2 cm^{-1} line of $PbTiS_3$ has the A_{1g} polarization characteristics, and then corresponds to the 335 cm^{-1} line of $1T$-TiS_2. The E_g mode of $PbTiS_3$ appears at around 225±4 cm^{-1} as a shoulder of the strong band at 194 cm^{-1}. This 225-cm^{-1} band is clearly separated from the 194-cm^{-1} band in the spectrum measured at 45 K and has the E_g polarization characteristics. Accordingly, the 225 cm^{-1} line of $PbTiS_3$ corresponds to the 235 cm^{-1} line of $1T$-TiS_2.

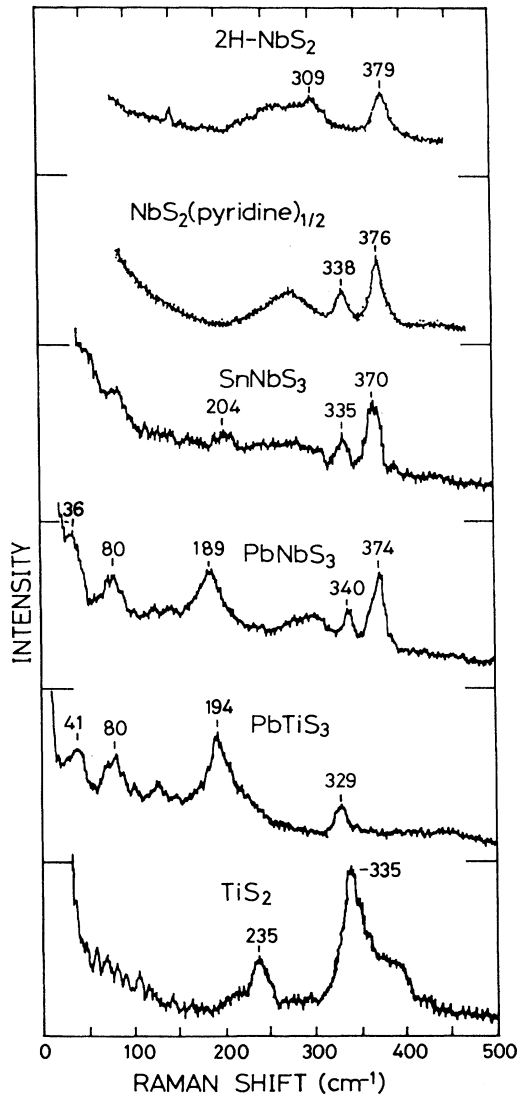

FIG. 2. Raman spectra of misfit-layer compounds, $SnNbS_3$, $PbNbS_3$, and $PbTiS_3$ measured at room temperature. Raman spectra of $2H$-NbS_2 and its intercalation compound $NbS_2(pyridine)_{1/2}$, and $1T$-TiS_2 are also shown for comparison.

The bands between 50 and 250 cm^{-1} are assigned to the intralayer modes of the MS layers. In the backscattering geometry two A_{1g} modes are allowed for the vibrational modes of the MS layer in MTS_3. It is evident that the spectra of $PbNbS_3$ and $PbTiS_3$ below 250 cm^{-1} are quite similar to each other. The 80±2 and 189±2 cm^{-1} (80±2 and 194±2 cm^{-1}) bands of $PbNbS_3$ ($PbTiS_3$) are assigned to the A_{1g} modes in the PbS layer. The 204±2 cm^{-1} band of $SnNbS_3$ is assigned to the A_{1g} intralayer vibration of the SnS layer. The first-order Raman scattering is allowed for the MS layer, although it is forbidden for the NaCl structure. The site symmetries of the atoms in the twofold atomic layers of MS cut out from the NaCl structure are low compared with those of the NaCl structure, and the first-order Raman scattering is allowed for the MS layer. The distortion from the NaCl structure in the MS layer also contributes to the appearance of the first-order Raman spectra for the MS layer.

Possible explanations for the origin of the 36±2 (41±2) cm^{-1} band of $PbNbS_3$ ($PbTiS_3$) are (1) the E_g mode in the PbS layer, (2) acoustic modes which become allowed in the incommensurate structure in the a direction, and (3) the rigid layer mode in which the MS and TiS_2 layers move as rigid bodies. The polarization vectors of the incident and scattered light lie in the ab plane in the backward scattering configuration on the c face used in this study. Since the symmetry of the PbS layer is approximated by the D_{4h} symmetry, the E_g modes, which are allowed for the (a',c) or (b',c) polarization, are forbidden in the backscattering configuration on the c face. Therefore, case (1) may be excluded. We tentatively assign the 36 (41) cm^{-1} band to the rigid layer mode because the E-like polarization characteristics are consistent with those of the shear-type rigid layer mode.

The above result indicates that the vibrational spectra of the TS_2 layers in MTS_3 are quite similar to those of the corresponding transition-metal disulfides. There are no Raman spectra of MS crystals which consist of twofold MS layers, but the Raman spectra of related compounds are available. SnS (α-SnS) crystallizes in the distorted NaCl structure and shows a number of modes below 300 cm^{-1} in the Raman spectra.[8] PbS crystallizes in the NaCl structure and the first-order scattering is forbidden. Brillson and Burstein[9] found a Raman band at 223 cm^{-1} in a PbS crystal overcoated by a thin Pb film, which is due to lowering of the symmetry by the internal electric field. The Raman spectra of the bulk SnS and overcoated PbS crystals are considerably different from those of the SnS and PbS layers in MTS_3. It will be reasonable to consider that the MS layer in MTS_3 has its own vibrational structure because the bonding between the atoms in the MS layer of MTS_3 is considerably different from those in the bulk MS crystals which have a three-dimensional bonding network. Comparison of the spectra of $PbNbS_3$ and $PbTiS_3$ indicates that the PbS layer has its characteristic vibrational structure irrespective of the species of the TS_2 layer, and that the Raman spectra of MTS_3 consist of the individual intralayer vibrations of the MS and TS_2 layers in the first approximation.

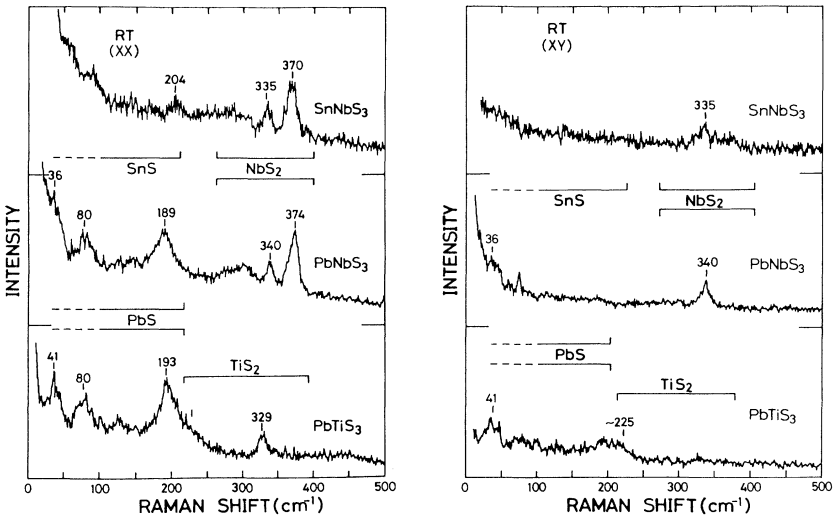

FIG. 3. Polarized (XX) and depolarized (XY) Raman spectra of $SnNbS_3$, $PbNbS_3$, and $PbTiS_3$.

B. Comparison with the intercalation compounds of TS_2

It is well known that the transition-metal dichalcogenides can be intercalated with various metal ions and organic molecules.[10,11] The intercalation reaction is believed to be promoted by the charge (electron) transfer from guests to the hosts (transition-metal dichalcogenides).[12] The change of Raman frequencies by intercalation has been investigated in several papers.[5,13–19] Nakashima *et al.*[5] compared the Raman frequencies of NbS_2 intercalated with various organic molecules with those of $2H$-NbS_2. They observed that the frequency of the E_{2g} mode shifts upwards by 20–30 cm^{-1} by the intercalation whereas the A_{1g} mode shows a slight downward shift. They attributed the shift of the E_{2g} modes to the charge transfer from the organic molecules to the NbS_2 layers. The ionic bonding between the host and guest molecules enhances the interlayer forces between the NbS_2 layers, which results in the upshift of the E_{2g} modes. The difference in the effect of the intercalation between the A_{1g} and E_{2g} modes has been attributed to the anisotropy of the long-range Coulomb interactions. The shift of the E_{2g} mode (E' mode in the D_{3h} symmetry) relative to that of the $2H$-NbS_2 crystal is +26 and +31 cm^{-1} for $SnNbS_3$ and $PbNbS_3$, respectively. The shift of the A_{1g} mode (A_1' mode in the D_{3h} symmetry) is rather small and amounts to −9 and −5 cm^{-1} for $SnNbS_3$ and $PbNbS_3$, respectively. These shifts cannot be attributed to the strain in the NbS_2 layer caused by the lattice matching between the NbS_2 and PbS (SnS) layers in the b direction: The lattice constants in the basal plane of the NbS_2 layers in $SnNbS_3$ and $PbNbS_3$ (the lattice constants corresponding to the trigonal structure) are slightly larger than those of $2H$-NbS_2.[1] Therefore, the downward shifts of the Raman frequencies are expected, which is opposite to the large upshifts observed for the E_{2g} mode.

It is reported that the frequency of the intralayer modes of NbS_2 are affected by the layer stacking. The A and E modes of $3R$-NbS_2 appear at 382 and 329 cm^{-1}, respectively[5] (MacMullan and Irwin[6] observed these modes at 386 and 330 cm^{-1} and Onari *et al.*[20] observed them at 382 and 325 cm^{-1}). Accordingly, the E and A modes shift by ~20 and ~3 cm^{-1}, respectively, on going from the $2H$ polytype to the $3R$ polytype. These upshifts of the intralayer modes are attributed to the stronger Nb-S force between adjacent layers for the $3R$ polytype than for the $2H$ polytype.[5] Although the upshifts of the E modes of $SnNbS_3$ and $PbNbS_3$ are comparable to that of the $3R$ polytype, the shifts of the A mode have opposite signs between $3R$-NbS_2 and $M$$NbS_3$.

The similarity of the shift of the Raman frequencies compared with $2H$-NbS_2 between NbS_2 intercalated with organic molecules and $M$$NbS_3$ suggests that the shift for these compounds should be explained in terms of the same mechanism. If we take into account that the interlayer interaction (interaction between the host and guest layers) may be quite different between NbS_2 intercalated with organic molecules and $M$$NbS_3$, it is reasonable to consider that the shift of the intralayer modes is caused by the change of the charge distribution in the NbS_2 layers due to the charge transfer from the guest layer to the NbS_2 layer. The occurrence of the charge transfer for $SnNbS_3$ is consistent with the conclusion deduced from the analysis of the XPS, XAS, and REELS measurements by Ohno.[4] The relationship between the amount of the charge transfer and the shift of the Raman frequency by the intercalation has not yet been studied systematically for the transition-metal dichalcogenides. The charge transfer for NbS_2 intercalated with pyridine has been estimated to be 0.2–0.3 electron per Nb atom by the NMR (Ref. 21) and optical transmission measurements.[22] The numbers of holes per one Nb atom estimated from the Hall coefficient are 0.88 and 0.20 for $SnNbS_3$ and $PbNbS_3$, respectively.[1] This means that the amount of the charge transfer is 0.12 and 0.80 per Nb for $SnNbS_3$ and $PbNbS_3$, respectively. The value for $SnNbS_3$ is reasonable if the shift of the intralayer mode can be taken as a measure of the amount of the charge transfer. However, the value of 0.80 for $PbNbS_3$ seems to be too large since the $SnNbS_3$ and $PbNbS_3$ show the similar frequency shifts of the intralayer modes.

The A_{1g} mode corresponding to the internal vibration

of the TiS_2 layer in $PbTiS_3$ appears at 329 cm^{-1}, which is 6 cm^{-1} lower than the frequency of the 1*T*-TiS_2 crystal. The frequency of the E_g mode of the TiS_2 layer is 225 cm^{-1} and is lower by 10 cm^{-1} compared with that of the 1*T*-TiS_2 crystal. This downward shift is too large to ascribe it to the strain caused by the partial lattice matching between the PbS and TiS_2 layers because the difference of the lattice constants in the *ab* plane of the TiS_2 layer (the lattice constants corresponding to the trigonal structure) in $PbTiS_3$ and that of 1*T*-TiS_2 is less than 0.2%.[1] The shift of the A_{1g} mode of TiS_2 upon the intercalation so far reported is small [+1 cm^{-1} for $LiTiS_2$ (Ref. 17) and +5 cm^{-1} for $Ag_{0.3}TiS_2$ (Ref. 14)]. The E_g mode shows negative shifts by the intercalation (−11 cm^{-1} for $LiTiS_2$ and −4 cm^{-1} for $Ag_{0.3}TiS_2$). The charge transfer from the PbS layer to the TiS_2 layer has been confirmed from the analysis of the XPS, XAS, and REELS spectra.[4] However, it is difficult, to decide whether the rather small shift of the intralayer modes of the TiS_2 layer is caused by the charge transfer or not.

The influence of the *M*S layer insertion into the van der Waals gap of TS_2 is larger for NbS_2 than TiS_2 (especially for the *E* mode). This fact implies larger interlayer interaction for $PbNbS_3$ and $SnNbS_3$ than $PbTiS_3$. According to the difference technique for XAS spectra, the interlayer interaction is stronger for $PbNbS_3$ and $SnNbS_3$ than $PbTiS_3$.[23]

The observed frequencies of the A_{1g} and E_{2g} (E_g) modes for MTS_3 are summarized in Table I together with those for pure TX_2 (X = S or Se) and their intercalation compounds. For TS_2 compounds with the trigonal prismatic coordination, there is a tendency that the frequency shift of the E_{2g} mode by the intercalation is positive and large whereas that of the A_{1g} mode is small. For TS_2 compounds with the octahedral coordination, on the other hand, the shift of the E_g mode is negative and that of the A_{1g} mode is small compared with the E_g mode. There is an empirical law that the Raman frequencies of the A_{1g} modes of metal dichalcogenides with CdI_2 and $CdCl_2$ structures plotted against the square of the characteristic frequencies $\Omega_0^2 = e^2/Mr_0^3$, where *e*, *M*, and r_0 are the elementary charge, reduced mass, and nearest-neighbor separation, respectively, are on a straight line.[19] The frequencies of the E_g modes are also on a straight line for the crystals which have anions belonging to the same group, whereas the slope of the line depends on the cation. This fact suggests that the frequencies of the E_g

TABLE I. Raman frequencies of MTS_3, TX_2 (X = S, Se), and intercalation compounds; in cm^{-1}.

Crystal	A_{1g}	$E_{2g}(E_g)$	Difference A_{1g}	Difference $E_{2g}(E_g)$	Ref.
2*H*-NbS_2	379	309			5
$SnNbS_3$	370	335	−9	+26	This work
$PbNbS_3$	374	340	−5	+31	This work
$NbS_2(pyridine)_{1/2}$	376	338	−3	+29	5
$NbS_2(aniline)_{1/2}$	378	330	−1	+21	5
$NbS_2(picoline)_{1/3}$	379	333	0	+24	5
2*H*-$NbSe_2$	228	237			16
$Fe_{1/4}NbSe_2$	228	250	0	+13	16
$NbSe_2(EDA)_{0.35}$	230	265	+2	+28	19
2*H*-TaS_2	400	286			24
$TaS_2(EDA)_{0.3}$	395	300	−5	+14	15
2*H*-$TaSe_2$	234	207			25
$TaSe_2(EDA)_p$	235	220	+1	+13	19
1*T*-TiS_2	335	235			This work
$PbTiS_3$	329	225	−6	−10	This work
$LiTiS_2$	336	224	+1	−11	17
$Ag_{0.3}TiS_2$	340	231	+5	−4	14
1*T*-ZrS_2	334	250			17
$LiZrS_2$	331	240	−3	−10	17
1*T*-HfS_2	337	257			17
$LiHfS_2$	340	238	+3	−19	17
1*T*-$TiSe_2$	198	135			17
$LiTiSe_2$	197	134	−1	−1	17
1*T*-$ZrSe_2$	195	146			17
$LiZrSe_2$	196	141	+1	−5	17

mode are affected by the effective charge of the cation, whereas those of the A_{1g} mode are little affected. We presume that the change of the effective charge of the Nb (Ti) ions due to the charge transfer from the MS layer to the Nb (Ti) ions of the NbS_2 (TiS_2) layer induces the change of the frequencies of the E modes through the long-range Coulomb interaction.

Pereira and Liang[16] proposed another interpretation of the different behavior between the A and E modes. They observed that the effect of the Fe intercalation into NbS_2 is different for the A_{1g} and E_{2g} modes. They explained it as follows: The electrons donated from the Fe atoms occupy the d_{z^2} orbitals of the Nb atoms. Since the main lobes of the d_{z^2} orbitals are in the z direction, the E-type phonon motions cause a change in the overlap between the sulfur valence orbitals and the partially filled d_{z^2} orbitals. The change of the occupation number of the d_{z^2} orbitals by the Fe intercalation causes the shift of the frequency of the E mode. On the other hand, the A-type phonon motion (displacement of the S atoms along the c axis) causes little change in the overlap, resulting in the small shift by the intercalation. However, these models cannot explain the difference of the sign of the shifts between the trigonal prismatic ($2H$) and octahedral coordination ($1T$) compounds for the E modes and further studies are needed to explain this difference.

C. Temperature dependence of Raman shift

Figures 4 and 5 show the temperature dependence of the Raman shifts for $SnNbS_3$ and $PbNbS_3$. In the figures, results are shown only for the relatively strong peaks. Large frequency variations of 8–9 and 13–15 cm^{-1} are observed for the A_{1g} and E_{2g} modes, respectively, in the NbS_2 layer for $SnNbS_3$ and $PbNbS_3$ in the range 30–300 K. The PbS vibrational modes at $\sim$200 cm^{-1} shift by $\sim$10 cm^{-1} with temperature when the sample is cooled from 300 to 30 K.

The shift of more than 8 cm^{-1} for the vibrational modes in the NbS_2 layer is considerably larger than those of MoS_2, which has the isostructural layer with NbS_2 [the shifts are 2.3 and 3.1 cm^{-1} for A_{1g} and E_{2g} modes, respectively, between 80 and 300 K (Ref. 26)]. One possible explanation for this large frequency shift with temperature is the effect of the fluctuation of the charge density wave (CDW). Tsang, Smith, and Shafer[27] observed large frequency variation even above the CDW transition temperature (T_c) for $2H$-$TaSe_2$ and -$NbSe_2$. They explained this result in terms of the interaction between the vibrational modes and the CDW state. Although the long-range order of the CDW disappears above T_c, the short-range localized CDW distortion (the CDW with a short correlation length) remains and the change of the localized CDW distortion with temperature induces the shift of the Raman bands.[27] The existence of the CDW has not been reported for $SnNbS_3$ and $PbNbS_3$ until now. However, the Fermi surfaces of these crystals may be unstable due to their two-dimensional nature and there is a possibility that the large shifts of the Raman frequency

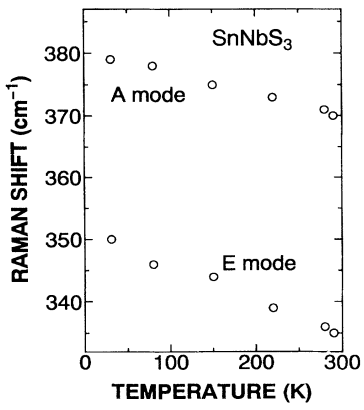

FIG. 4. Temperature dependence of the frequencies of the NbS_2 intralayer vibrational modes for $SnNbS_3$.

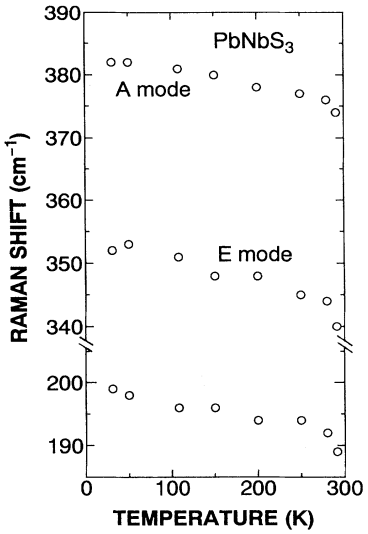

FIG. 5. Temperature dependence of the frequencies of some vibrational modes for $PbNbS_3$.

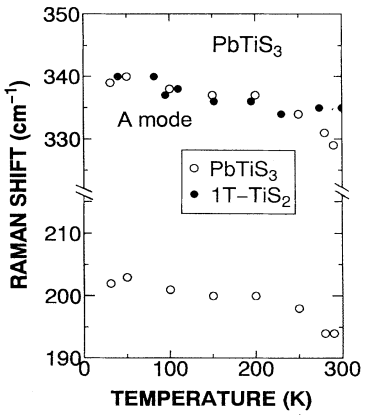

FIG. 6. Temperature dependence of the frequencies of some vibrational modes for $PbTiS_3$ (open circles). The temperature dependence of the frequency of the A_{1g} mode of $1T$-TiS_2 is also shown for comparison (closed circles).

with temperature in $SnNbS_3$ and $PbNbS_3$ are related to the existence of the localized CDW distortion which is a precursor of the static CDW distortion with long-range order.

Figure 6 shows the temperature dependence of the Raman shifts for $PbTiS_3$. For comparison the temperature dependence of the A_{1g} mode of the $1T$-TiS_2 crystal is also shown in Fig. 6. The shift of the A_{1g} mode of $PbTiS_3$ in the temperature range 30–300 K is 10 cm^{-1}. The shift of the A_{1g} mode of $1T$-TiS_2 with temperature is consistent with that reported by Sandoval, Chen, and Irwin.[28] The frequency variation of the A_{1g} mode for $PbTiS_3$ is somewhat larger than that for the $1T$-TiS_2 crystal. The change of the frequency of the A_{1g} mode of the isostructural insulator HfS_2 between 77 K and room temperature is only 2 cm^{-1}.[29] $1T$-TiS_2 is a dirty semiconductor and does not undergo the CDW phase transition. However, recent observations by scanning tunneling microscopy demonstrate the existence of the localized CDW in $1T$-TiS_2.[30] The large frequency shift of the TiS_2 intralayer modes observed for $1T$-TiS_2 and $PbTiS_3$ may be interpreted in terms of the interaction of the phonon modes with the localized CDW as for $SnNbS_3$ and $PbNbS_3$.

V. SUMMARY

Raman-scattering spectra have been measured for the misfit-layer compounds MTS_3 ($SnNbS_3$, $PbNbS_3$, and $PbTiS_3$). The spectra are regarded as the superposition of the individual vibrational spectra of the MS and TS_2 layers. This result indicates a weak interlayer interaction in these materials. The peaks at around 40 cm^{-1} observed for $PbNbS_3$ and $PbTiS_3$ are assigned tentatively to the rigid layer mode. The Raman frequency for the intralayer vibrations of the NbS_2 layers deviates from that of the NbS_2 crystals, which leads to the conclusion that the charge transfer from the MS layer to the NbS_2 layer occurs. From the comparison with Raman frequencies of various intercalation compounds of transition-metal dichalcogenides, it is found that the insertion of guest layers between the MX_2 (X = S, Se) layers changes the E-type mode frequency considerably, whereas it hardly changes the A-type mode frequency. It is also found that the change of the E-mode frequency by the insertion of guest layers has different sign for the compounds with trigonal prismatic and octahedral configurations. The noticeable change in the Raman frequencies with temperature for $SnNbS_3$, $PbNbS_3$, and $PbTiS_3$ may be associated with the precursor of the static CDW distortion.

*Present address: Research Center for Superconducting Materials and Electronics, Osaka University, Suita, Osaka 565, Japan.

†Present address: Dainippon Screen Mfg. Co. Ltd., Kamigyo-ku, Kyoto 602, Japan.

[1]G. A. Wiegers and A. Meerschaut, in *Incommensurate Sandwich Layered Compounds,* edited by A. Meerschaut (Trans. Tech. Publ., Aedermannsdorf, Switzerland, 1992), p. 101.

[2]G. A. Wiegers, A. Meetsma, R. J. Haange, and J. L. de Boer, Mater. Res. Bull. **23**, 1551 (1988).

[3]G. A. Wiegers, A. Meetsma, R. J. Haange, and J. L. de Boer, Solid State Ionics **32/33**, 183 (1989).

[4]Y. Ohno, Phys. Rev. B **44**, 1281 (1991).

[5]S. Nakashima, Y. Tokuda, A. Mitsuishi, R. Aoki, and Y. Hamaue, Solid State Commun. **42**, 601 (1982).

[6]W. G. McMullan and J. C. Irwin, Solid State Commun. **45**, 557 (1983).

[7]J. E. Smith, Jr., M. I. Nathan, M. I. Shafer, and J. B. Torrance, in *Proceedings of the 11th International Conference on the Physics of Semiconductors,* edited by M. Miąsek (PWN–Polish Scientific Publishers, Warsaw, 1972), p. 1306.

[8]H. R. Chandrasekhar, R. G. Humphreys, U. Zwick, and M. Cardona, Phys. Rev. B **15**, 2177 (1977).

[9]L. Brillson and E. Burstein, in *Proceedings of the 2nd International Conference on Light Scattering in Solids,* edited by M. Balkanski (Flammarion Sciences, Paris, 1971), p. 320.

[10]G. V. Subba Rao and M. W. Shafer, in *Intercalated Layered Materials,* edited by F. Levy (Reidel, Dordrecht, 1979), p. 99.

[11]R. H. Friend and A. D. Yoffe, Adv. Phys. **36**, 1 (1987).

[12]J. V. Acrivos and J. R. Salem, Philos. Mag. **30**, 603 (1974).

[13]J. C. Tsang and M. W. Shafer, Solid State Commun. **25**, 999 (1978).

[14]W. K. Unger, J. M. Reyes, O. Singh, A. E. Curzon, J. C. Irwin, and R. F. Frindt, Solid State Commun. **28**, 109 (1978).

[15]M. Hangyo, S. Nakashima, and A. Mitsuishi, Ferroelectrics **52**, 151 (1983).

[16]C. M. Pereira and W. Y. Liang, J. Phys. C **18**, 6075 (1985).

[17]P. C. Klipstein, C. M. Pereira, and R. H. Friend, Philos. Mag. B **56**, 531 (1987).

[18]W. G. McMullan and J. C. Irwin, Can. J. Phys. **62**, 789 (1984).

[19]S. Nakashima, M. Hangyo, and A. Mitsuishi, in *Vibrational Spectra and Structure,* edited by J. R. Durig (Elsevier, Amsterdam, 1985), Vol. 14, p. 305.

[20]S. Onari, T. Arai, R. Aoki, and S. Nakamura, Solid State Commun. **31**, 577 (1979).

[21]E. Ehrenfreund, A. C. Gossard, and F. R. Gamble, Phys. Rev. B **5**, 1708 (1972).

[22]A. R. Beal and W. Y. Liang, J. Phys. C **6**, L482 (1973).

[23]Y. Ohno, Solid State Commun. **79**, 1081 (1991).

[24]S. Sugai, K. Murase, S. Uchida, and S. Tanaka, Solid State Commun. **40**, 399 (1981).

[25]J. A. Holy, M. V. Klein, W. L. McMillan, and S. F. Meyer, Phys. Rev. Lett. **37**, 399 (1976).

[26]J. M. Chen and C. S. Wang, Solid State Commun. **14**, 857 (1974).

[27]J. C. Tsang, J. E. Smith, Jr., and M. W. Shafer, Solid State Commun. **27**, 145 (1978).

[28]S. Jiménez Sandoval, X. K. Chen, and J. C. Irwin, Phys. Rev. B **45**, 14 347 (1992).

[29]T. Iwasaki, N. Kuroda, and Y. Nishina, J. Phys. Soc. Jpn. **51**, 2233 (1982).

[30]G. P. E. M. Van Bakel and J. Th. M. De Hosson, Phys. Rev. B **46**, 2001 (1992).